

tially zero temperature dependency of the blend films is consistent with that of the pure conducting polymers. The growth of PPy and PTh has been studied by SEM. The morphology of the films may be related to the potential applied to the system,<sup>9</sup> the film thickness of insulating polymer coated on the electrode, and the physical and chemical interactions between conducting and insulating polymers. Since there are only a limited number of conducting polymers, the above information is encouraging and suggests that polymer blends may continue to offer a route to improve physical properties in conducting polymers.

**Acknowledgment.** We thank the Fulbright Commission for a grant to L.T. which made it possible for him to visit the University of South Florida. We also acknowledge the support of the USF Division of Sponsored Research, helpful suggestions by Michael Randazzo, and DSC and TGA scans by Kusay Al-Jumah of the University of Florida.

## References and Notes

- (1) Bargon, J.; Mohmand, S.; Waltman, R. J. *IBM J. Res. Dev.* **1981**, *25*, 51.
- (2) Diaz, A. F.; Kanazawa, K. K.; Gardini, G. P. *J. Chem. Soc., Chem. Commun.* **1979**, 635.
- (3) Diaz, A. F.; Kanazawa, K. K. *Chem. Scr.* **1981**, *17*, 45.
- (4) Tourillon, G.; Garnier, F. J. *Electroanal. Chem.* **1982**, *135*, 173.

- (5) Diaz, A. F.; Hall, B. *IBM J. Res. Dev.* **1983**, *27*, 342.
- (6) Niwa, O.; Tamamura, T. *J. Chem. Soc., Chem. Commun.* **1984**, 817.
- (7) De Paoli, M.; Waltman, R. J.; Diaz, A. F.; Bargon, J. *J. Chem. Soc., Chem. Commun.* **1984**, 1015.
- (8) De Paoli, M.-A.; Waltman, R. J.; Diaz, A. F.; Bargon, J. *J. Polym. Sci., Polym. Chem. Ed.* **1985**, *23*, 1687.
- (9) Niwa, O.; Tamamura, T.; Kakuchi, M. *Macromolecules* **1987**, *20*, 749.
- (10) Nagasubramanian, G.; DiStefano, S. J. *Electrochem. Soc. Extended Abstr.* **1985**, *85-2*, 659.
- (11) Zallen, R. *The Physics of Amorphous Solids*; Wiley: New York, **1983**; Chapter 4.
- (12) Aldissi, M.; Bishop, A. R. *Polymer* **1985**, *26*, 622.
- (13) Hotta, S.; Rughooputh, S. D. D. V.; Heeger, A. J. *Synth. Met.* **1987**, *22I*, 79.
- (14) Toppare, L.; Eren, S.; Ozel, O.; Akbulut, U. *J. Macromol. Sci., Chem.* **1984**, *A21(10)*, 1281.
- (15) Waltman, R. J.; Bargon, J.; Diaz, A. F. *J. Phys. Chem.* **1983**, *87*, 1459.
- (16) Shrieffer, D. F.; Farrington, G. C. *Chem. Eng. News* **1985**, *63(20)*, 42.
- (17) Brandup, J.; Immergut, E. H. *Polymer Handbook*; Wiley: Sons, New York, **1975**.
- (18) Coleman, M. M.; Shrovanek, D. J.; Hu, J.; Painter, P. C. *Macromolecules* **1988**, *21*, 59.
- (19) Street, G. B.; Clarke, T. C.; Krounki, M.; Kanazawa, K.; Lee, V.; Pfluger, P.; Scott, J. C.; Weiser, G. *IBM Res. Div. Rep.* **1981**, *RJ3267(39723)*, 1.

**Registry No.** PS, 9003-53-6; (PC)(bisphenol A) (copolymer), 25037-45-0; (PC)(bisphenol A) (SRU), 24936-68-3; PPy, 30604-81-0; PTh, 25233-34-5.

## A Novel Micellar Synthesis and Photophysical Characterization of Water-Soluble Acrylamide-Styrene Block Copolymers

Kenneth C. Dowling and J. K. Thomas\*

Department of Chemistry, University of Notre Dame, Notre Dame, Indiana 46556.  
Received June 6, 1989; Revised Manuscript Received July 27, 1989

**ABSTRACT:** A novel micellar polymerization was utilized in the one-step synthesis of water-soluble block copolymers of acrylamide and styrene and in the control of styrene block sizes in the predominantly acrylamide polymer chain. Block sizes were determined from Poisson fluorescence quenching kinetics and ranged from 14 to 30 styrenes. Fine structure in pyrene probe fluorescence revealed that the blocks impart hydrophobic domains to aqueous copolymer solutions. Fluorescence quenching was monitored to determine that the copolymers isolate and screen hydrophobic molecules from the aqueous phase. A coiled configuration of the polyacrylamide backbone about the styrene blocks is shown to be a contributor to the screening effect.

## Introduction

Photophysical and photochemical investigations of organized molecular assemblies such as micelles, vesicles, and bilayers, including polymeric systems, have received much attention in recent literature.<sup>1-4</sup> The ability of such systems to provide unique environments for reactions as well as their suitability for modeling certain biological systems yields a variety of potential applications, e.g. drug encapsulation, solar energy conversion, and catalysis.<sup>1,5</sup> Recently, amphiphilic polymers have become the focus of extensive research<sup>6-8</sup> for their ability to impart a greater degree of organization compared to homogeneous systems. The potential to tailor amphiphilic polymers to specific systems warrants the continued exploration of these materials.

Copolymerization of a hydrophobic monomer with a hydrophilic monomer can result in an amphiphilic polymer, the specific nature of which can be controlled via polymerization parameters. The dual hydrophilic/hydrophobic nature provides these materials with unique solubilization characteristics and modifies physical properties of the bulk polymer.<sup>9</sup> Water-soluble amphiphilic polymers are of particular interest as a chemical system due to the presence of microdomains that may impart unusual reactivity to a given chemical system. In this paper we describe our work on acrylamide-styrene copolymers that provide hydrophobic sites in aqueous solutions.

Earlier studies have demonstrated the applicability of micellar polymerization for controlling polystyrene latex particle sizes.<sup>10,11</sup> In the present study, the micellar polymerization of styrene is carried out in an aqueous solution of acrylamide to form the water-soluble copoly-

\* To whom correspondence should be addressed.

Table I  
Copolymerizations of Acrylamide and Styrene

copolymer	[sty], mM	[AM], M	[AIBN], mM	[CTAB], mM	[sty]/[micelle] <sup>a</sup>	[AM]/[Sty]	solubility
random <sup>b</sup>	19.6	0.717	1.08			37	yes
P(AM/Sty)-13	17.3	0.707	1.46	80.5	13	41	yes
P(AM/Sty)-22	17.3	0.711	0.87	52.1	22	41	yes
P(AM/Sty)-28	17.4	0.707	0.66	37.8	28	41	yes
P(AM/Sty)-37	17.4	0.707	0.56	28.0	37	41	partial
P(AM/Sty)-47	17.3	0.707	0.40	22.2	47	41	marginal
P(AM/Sty)-58	17.4	0.707	0.39	18.0	58	41	no

<sup>a</sup> Calculated from CTAB aggregation number  $\bar{N} = 60$  and cmc =  $9.2 \times 10^{-4}$  M.<sup>19</sup> <sup>b</sup> Polymerized in 1,4-dioxane; all others in aqueous solutions.

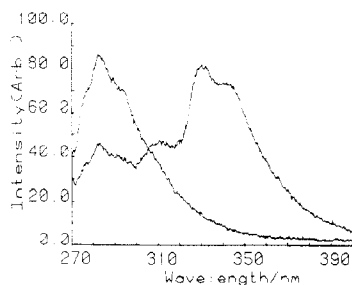


**Figure 1.** Fluorescent emission spectra from P(AM/STY) copolymers: excitation wavelength, 260 nm; random copolymer (3.1 g/L) exhibits only monomer emission;  $\lambda_{\max} = 283$  nm. Block copolymer P(AM/STY)-28 (3.2 g/L) exhibits primarily excimer emission:  $\lambda_{\max} = 332$  nm.

mers. This technique offers the advantage of being a one-step copolymerization allowing isolation of the hydrophobic styrene monomers and hydrophilic acrylamide monomers during the reaction. The characterization of these copolymers is described in this report and relies primarily on photophysical phenomena. The main goal of the present work is to synthesize and characterize water-soluble acrylamide-styrene (AM/Sty) block copolymers and to characterize the resultant chemical environments of solubilized hydrophobic probes.

## Experimental Section

**Materials.** Electrophoresis grade acrylamide was used as received from Aldrich Chemicals. Styrene from Eastman was vacuum distilled prior to use. Hexadecyltriethylammonium bromide (CTAB) was obtained from Sigma Chemical Co. and recrystallized twice from absolute ethanol. *N,N*-Dibutylaniline (DBA) and nitromethane from Eastman Kodak Co. were distilled twice under vacuum prior to use. 2,2'-Azobis(2-methylpropionitrile) (AIBN) from Aldrich was twice recrystallized from methanol. The pyrene used was obtained from Sigma Chemical Co. and was purified by column chromatography prior to use. All other chemicals were reagent grade and used as received. Distilled, deionized water was used exclusively for all aqueous solutions.

**Equipment.** Steady-state fluorescence measurements were conducted on Perkin-Elmer MPF 44B and SLM-Aminco SPF-500C spectrofluorometers. UV-visible Absorption spectra were measured on a Perkin-Elmer 551 spectrophotometer. Time-resolved transient fluorescence decays were obtained by using a PRA Nitromite Laser for excitation pulses a 337.1 nm (120 ps, 30- $\mu$ J pulse). A Tektronix 7912 AD transient capture device was used to collect emission data that were subsequently processed on a Zenith PC. Details of the experimental laser flash equipment used are as described previously.<sup>4,12</sup>

**Synthesis of Copolymers.** The copolymers used in this investigation were prepared in aqueous solution by micellar polymerization using CTAB as the supporting surfactant. Reaction mixtures are provided in Table I. The CTAB aggregation number may increase with the addition of styrene, and therefore calculated occupancies are provided only for comparison.<sup>11</sup> In addition, a random AM/Sty copolymer was prepared by precipitation polymerization from dioxane with an acrylamide, styrene, and AIBN homogenous solution. Reaction

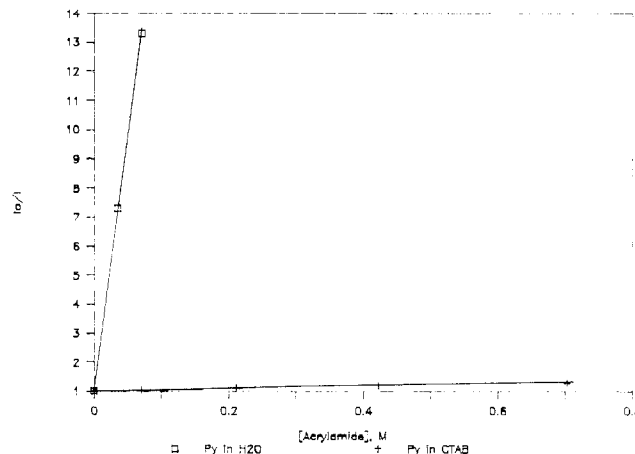


**Figure 2.** Quenching of pyrene by acrylamide. Pyrene in a saturated aqueous solution ( $3 \times 10^{-7}$  M) yields a steep slope indicating efficient quenching by acrylamide. Pyrene in a  $5.2 \times 10^{-2}$  M CTAB micellar solution (concentration comparable to that in reaction mixtures) exhibits very inefficient quenching by acrylamide, indicating that penetration by the acrylamide monomer is nominal.

mixtures were placed in 50-mL Erlenmeyer flasks covered with septum caps and were degassed by gentle bubbling with styrene-saturated nitrogen gas for 15 min. The mixtures were then irradiated in a Rayonet photoreactor<sup>11</sup> with 300-nm minimum wavelength white light for 1.5 h without agitation, followed by 12 h in darkness. Polymers were then recovered by precipitation with the addition of methanol. The polymers were repeatedly dissolved in water, precipitated, and washed several times with copious amounts of methanol, thus removing CTAB and unreacted monomers from the finished polymers. Copolymers were hydrolyzed in aqueous solutions of 40 g/L copolymer and 1 M NaOH providing nearly 2:1 excess base. Solutions were held at 80 °C for 18 h, and the resulting hydrolyzed polymers were precipitated and washed as above. The degree of hydrolysis was not analytically determined but is expected to be high and sufficient for the studies used later in the paper.

## Results and Discussion

The molecular weights of the polymers are estimated to be  $3 \times 10^5$  from the following relationship<sup>13</sup>

$$[\eta]/100 \text{ cm}^3/\text{g} = 6.8 \times 10^{-4} M_w^{0.66}$$

assuming the copolymers behave similar to the homopolymer polyacrylamide.

**Styrene Configuration.** The acrylamide-styrene copolymers, P(AM/Sty), that were soluble in water each exhibited measurable fluorescent emission from the pendant phenyl groups. Steady-state fluorescence spectra of aqueous solutions of the P(AM/Sty) copolymers were measured in an effort to confirm the "block nature" of the styrene incorporated in the predominantly acrylamide polymer backbone. Figure 1 compares spectra of a random AM/Sty copolymer and the block copolymer P(AM/Sty)-28 (see Table I) prepared via micellar copo-

lymerization. It is evident from these spectra that the random copolymer exhibits only monomer emission similar to that of dilute polystyrene solutions (peak centered at 283 nm), whereas the micellar produced AM/Sty copolymer exhibits a combination of monomer and excimer emission (excimer peak centered at 331 nm). The excimer emission is reminiscent of that of polystyrene films, a result of the close packing of the pendant phenyl groups. In the aqueous solutions of the AM/Sty copolymers, the excimer emission is thus indicative of the presence of styrene blocks in the polymer. The polymers are not true block copolymers in that there is probably a significant amount of styrene at positions with only acrylamide as nearest neighbors as evidenced by the nonnegligible styrene monomer emission from these copolymers.

The styrene in monomer positions can be accounted for in the reaction mechanism by the small amounts of aqueous styrene and the penetration of the micelle by acrylamide. Such penetration of the micelle is small but nonnegligible at 0.7 M acrylamide, as seen in the quenching of micellized pyrene fluorescence by acrylamide in Figure 2. The acrylamide monomer is an efficient quencher of pyrene fluorescence as evident in the pyrene/water system ( $k_q = 8 \times 10^8 \text{ M}^{-1} \text{ s}^{-1}$ ). In the presence of CTAB micelles, the quenching interactions are largely inhibited as evident from the decrease in quenching observed ( $k_q = 1.1 \times 10^6 \text{ M}^{-1} \text{ s}^{-1}$ ). Thus, it is inferred that the acrylamide monomer resides all but exclusively in the aqueous phase and only minor amounts are expected to react in the polymerization within the micelles. Conversely, the limited solubility of styrene in water suggests the styrene would be predominantly polymerized within the micelles. The observed styrene fluorescence from the resulting polymers (Figure 1) is consistent with the preceding arguments.

**Probe Studies of Host Sites.** The next step in the characterization of these polymers required the addition of the environment-sensitive probe pyrene to the solutions of the AM/Sty copolymers. The utility of fluorescence probes in the investigation of organized assemblies has been demonstrated.<sup>14</sup> The variation of the fine structure in the fluorescence of pyrene, in particular the ratio of the III peak to the I peak, is well documented.<sup>15</sup> In hydrophobic media large III/I values are expected, and small values are expected in polar or highly perturbing media. Figure 3 presents the pyrene spectra in (A) water, (B) micellar CTAB, (C) random AM/Sty copolymer, and (D) P(AM/Sty)-28 block AM/Sty copolymer. It is apparent from the III/I ratios that in the random copolymers, pyrene experiences an environment similar to that in water. The block copolymer solutions, however, provide hydrophobic sites for the solubilization of pyrene as the III/I ratios are similar to those found in the hydrophobic domains of the micelles. No hydrophobic domains are evident in polyacrylamide solutions or in the random AM/Sty copolymers. In addition, the block copolymers solubilize up to 300 times more pyrene ( $3 \times 10^{-5} \text{ M}$ ) in a 3 g/L solution than the random copolymer. This evidence confirms the hydrophobic nature imparted to the block copolymer solutions as a result of the styrene blocks produced in the micellar polymerization.

The hydrophobic sites resulting from the AM/Sty block copolymers appear to be fundamentally different from normal micelles despite the similarities in pyrene III/I ratios. The copolymer sites are stable to extreme dilution, but micelles generally are an aggregation of amphiphilic molecules that dissociate when diluted below a critical concentration. The dilution stability can be

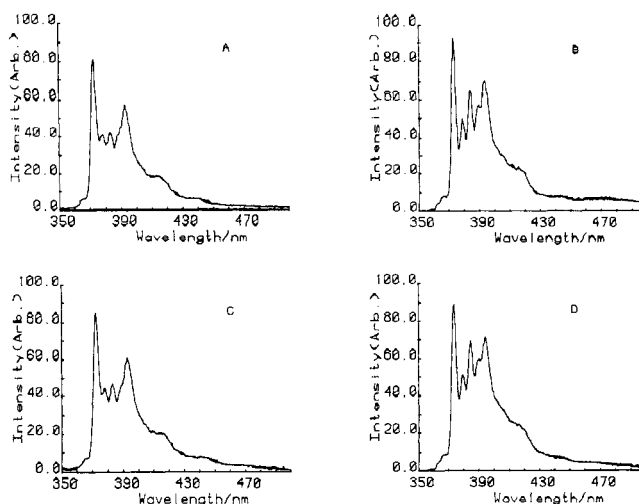


**Figure 3.** Pyrene emission spectra in various media. Clockwise from top left: (A)  $3 \times 10^{-7} \text{ M}$  pyrene in water, III/I = 0.52; (B)  $1 \times 10^{-6} \text{ M}$  pyrene in  $5 \times 10^{-2} \text{ M}$  CTAB (hydrophobic regimes provided by micelles), III/I = 0.72; (C)  $3 \times 10^{-7} \text{ M}$  pyrene in random P(AM/STY) copolymer (4 g/L), III/I = 0.53; (D)  $1 \times 10^{-5} \text{ M}$  pyrene in P(AM/STY)-28 block copolymer (3 g/L), III/I = 0.77. Excitation wavelength: 337 nm.

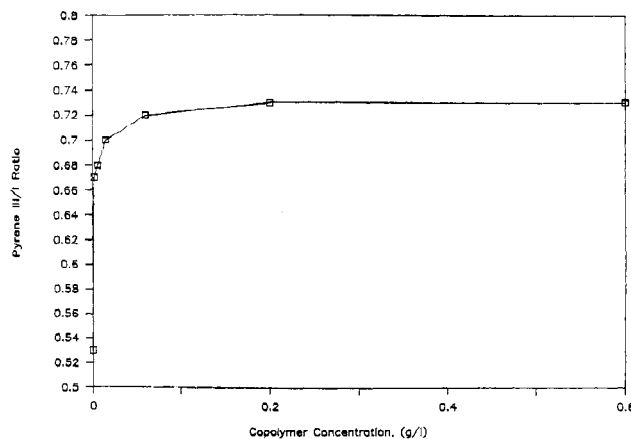


**Figure 4.** Dilution stability of hydrophobic sites in P(AM/STY)-22 block copolymer. Pyrene concentrations range from  $1 \times 10^{-6} \text{ M}$  in 0.6 g/L copolymer solution to  $3 \times 10^{-7} \text{ M}$  in most dilute solutions.

seen from the plot of pyrene III/I ratios versus copolymer concentration in Figure 4. The ratio remains constant to  $\sim 0.1 \text{ g/L}$  copolymer which corresponds to  $3 \times 10^{-5} \text{ M}$  in styrene and  $5 \times 10^{-7} \text{ M}$  pyrene (maximum pyrene at this polymer concentration). The slight decrease in III/I ratios below 0.1 g/L is attributed to the distribution of pyrene between the sites and the water. At these low pyrene concentrations, the fluorescence signal detected from pyrene in the water provides a significant contribution to the overall measured spectrum. Yet, even at 0.002 g/L the III/I ratios are substantially higher than those observed in water alone (0.67 vs 0.53). It is important to note that the contribution to the signal from site-solubilized pyrene will in general be greater per pyrene due to the longer fluorescence lifetime in a hydrophobic medium. Nevertheless, it is concluded that the hydrophobic domains are a direct result of the styrene blocks present in the micellar-polymerized copolymers as opposed to an aggregation of said sites since they continue to solvate pyrene at extreme dilution. Consequently, these sites may be regarded as a type of intramolecular micelle.

**Quenching Studies of Host Sites.** Fluorescence quenching measurements of pyrene solubilized in the

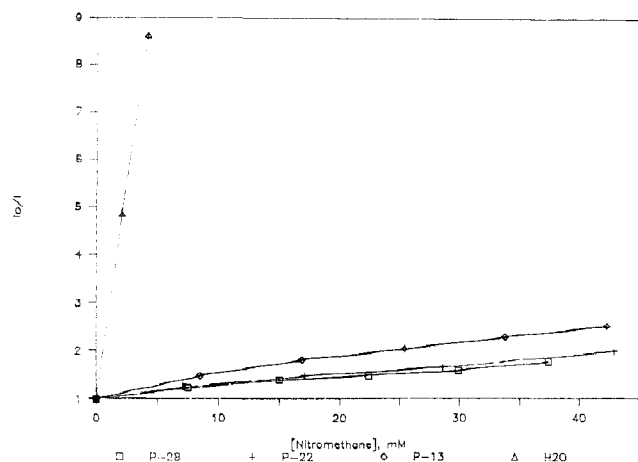


**Figure 5.** Quenching of pyrene by nitromethane in P(AM/STY) block copolymers and water. Copolymer solutions of various block sizes are each 2.6 g/L copolymer and  $7.7 \times 10^{-6}$  M pyrene. Quenching in water is measured in a  $3 \times 10^{-7}$  M pyrene solution. Block size is relatively unimportant in the screening of pyrene from the polar quencher, nitromethane.

**Table II**  
Styrene Block Sizes from Poisson Model

copolymer	$\bar{N}$ , Sty/site		$10^{-6} k_0$ , $s^{-1}$	$10^{-7} k_q$ , $s^{-1}$
	steady state	transient		
P(AM/Sty)-13	15	14	3.27	1.28
P(AM/Sty)-22	21	19	3.05	1.00
P(AM/Sty)-28	28	25	3.33	1.11
P(AA/Sty)-37	34	30	3.10	2.74

hydrophobic sites of the block AM/Sty copolymers were performed to gain information regarding the nature of the site. The ionic quenchers  $I^-$  and  $Tl^+$  that readily quench pyrene fluorescence in homogeneous solutions have virtually no effect on the intensity of the steady-state pyrene fluorescence (nor fluorescence lifetimes) in block copolymer solutions. In addition, the quenching efficiency of the polar quencher nitromethane is greatly reduced. Results of the steady-state quenching by nitromethane are presented in the form of a Stern-Volmer plot in Figure 5 for pyrene in water and pyrene in the block copolymers. The nominal curvature is evidence of more than one environment for probe solvation as discussed later. However, all the block copolymers showed a marked decrease in the accessibility of solubilized pyrene by nitromethane. Consequently, it is concluded that each copolymer has hydrophobic sites that are either relatively large or restrictive of solute mobility in order to inhibit the quencher-probe interactions.

**Rigidity of Sites.** Fluorescence depolarization experiments can provide qualitative information regarding the rigidity of the environment experienced by the pyrene molecules. The degree of polarization,  $P$ , is defined:

$$P = \frac{I_{ee} - (I_{eb}/I_{bb})I_{be}}{I_{ee} + (I_{eb}/I_{bb})I_{be}}$$

The subscripts e and b indicated orientation of the polarizer for the measured fluorescence intensities (see ref 16 for a more detailed discussion of fluorescence depolarization measurements). In a rigid medium (methylcyclohexane glass) the degree of polarization for 9-methylanthracene was measured to be  $P = 0.14$  from steady-state fluorescence intensities. In a fluid medium (methylcyclohexane) it was measured as 0.00. Solubilized in an aqueous solution of the block copolymer P(AM/Sty)-22, steady-state 9-methylanthracene depolarization measurements yield a high degree of polarization,  $P$

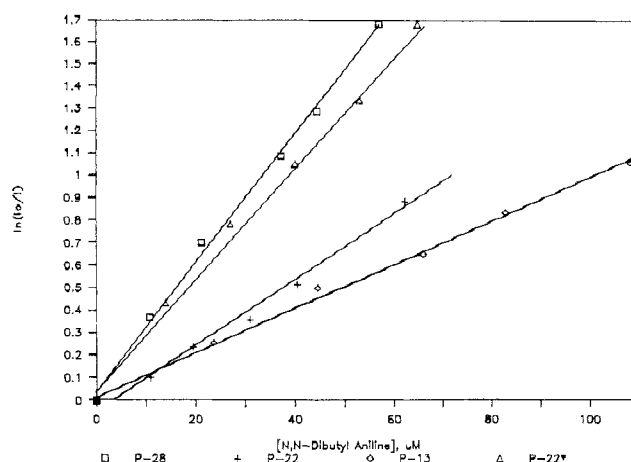


**Figure 6.** Steady-state quenching of pyrene by *N,N*-dibutylaniline in P(AM/STY) block copolymer solutions. P-28, P-22, and P-13 are 4 g/L and P-22\* is 3 g/L; each with  $5 \times 10^{-6}$  M pyrene. By the Poisson model,  $\ln(I_0/I)$  vs [DBA] is linear with slope  $= 1/[\text{sites}]$ . Values for  $N$  calculated are as follows: (a) P-28,  $N = 28$ ; (b) P-22,  $N = 21$ ; (c) P-13,  $N = 15$ ; and (d) P-22\*,  $N = 20$ .

$= 0.13$ , tending to indicate that reorientation of the 9-methylanthracene molecule on the time scale of fluorescence lifetimes is largely prohibited. It is reasonable to assume that sites that hinder 9-methylanthracene motion also inhibit pyrene mobility, as the relatively long lifetime of pyrene fluorescence induces depolarization in steady-state polarization measurements due to the mobility of solubilizing sites on the time scale of fluorescence. The protective nature of the hydrophobic sites can be partially attributed to an inhibited mobility of solutes, which should be expected for sites arising from the close packing of polystyrene phenyl groups in an aqueous medium which were demonstrated.

**Size of Host Sites.** Attempts to determine the sizes of hydrophobic sites in the block copolymers using SEM or dynamic light scattering were not fruitful in that the polyacrylamide backbone interferes with the measurements. Fortunately, photophysical techniques are applicable to this problem as explained below. Hydrophobic quenchers, unlike polar quenchers, distribute preferentially to the hydrophobic sites of the styrene blocks. In aqueous micellar solutions a Poisson distribution of hydrophobic quenchers has been demonstrated to be the only model to describe these systems.<sup>4</sup> The similarity of the block copolymer solutions to micelles suggests that the Poisson distribution should be applicable. If probe concentrations are low and the distribution of quenchers among the available sites can be approximated by a Poisson distribution, the fluorescence quenching kinetics take on the following form

$$I_F(t) = I_F(0) \exp\{-k_0 t - n[1 - \exp(-k_q t)]\}$$

where  $I_F(0)$  and  $I_F(t)$  are the initial and time-dependent fluorescence intensities, respectively. In absence of added quenchers, the decay rate constant is given by  $k_0$ ;  $k_q$  is the fast quenching rate constant as a result of quenchers in the microdomain with the probe; and  $n$  is the average number of quenchers per site,  $[Q]/[\text{site}]$ . The steady-state fluorescence should then follow:<sup>17</sup>

$$I/I_0 = \exp(-n) \sum_{i=0}^{\infty} \frac{n^i}{i!} [1 + i(k_q/k_0)] \sim \exp(-[Q]/[\text{site}])$$

Thus, a plot of  $\ln(I_0/I)$  vs  $[Q]$  should be a straight line with a slope equal to  $1/[\text{site}]$ , allowing the calculation of site concentrations. Consequently the average number of sty-

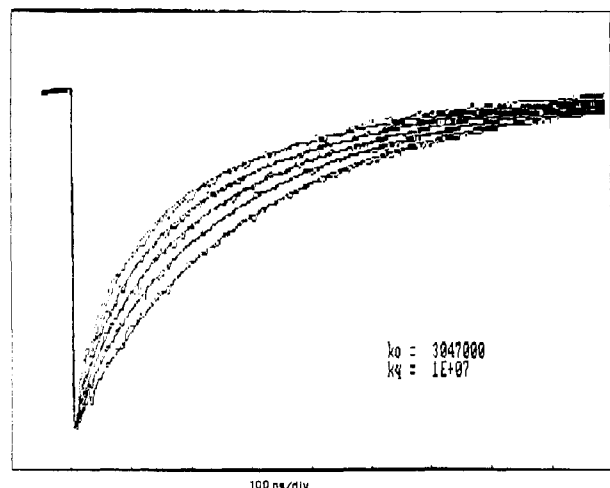


**Figure 7.** Curve fitting of transient decays to Poisson kinetics. Shown are the fluorescence decays for  $5 \times 10^{-6}$  M pyrene in 4 g/L P(AM/STY)-22 block copolymer with  $(0-6) \times 10^{-5}$  M DBA along with appropriate Poisson fits. Parameters:  $k_0 = 3.05 \times 10^6$  s $^{-1}$ ;  $k_q = 1.00 \times 10^7$  s $^{-1}$ ;  $n$  varies as a function of quencher concentration. Emission monitored at 400 nm.

renes per site,  $N$ , is calculated from the styrene concentration in the solution which is easily determined from the UV-vis absorption spectrum. Values of  $n$  may be calculated for comparison with the  $n$  values determined from curve fitting of the transient fluorescence decays.

Several hydrophobic quenchers of pyrene emission were used in an effort to observe Poisson kinetics in the copolymers. 1-Nitrododecane and  $N,N$ -dibutylaniline gave the best fits of the transient decays to the Poisson scheme. Only the results from the DBA quenching are reported here because while DBA concentrations are easily monitored by its absorption at 305 nm, the concentrations of 1-nitrododecane were impossible to monitor and difficult to prepare reproducibly. Figure 6 shows the steady-state quenching of pyrene in block copolymers P(AM/Sty)-13, P(AM/Sty)-22, and P(AM/Sty)-28. The slopes of these plots yield estimates for the average styrenes per site ratios that are summarized in Table II. Time-resolved fluorescence decays, shown in Figure 7, justify the use of the Poisson scheme to analyze the quenching by DBA. At short times the decay rate is increased as quencher concentration increases due to a higher proportion of probed sites that also contain a quencher. The relatively fast quenching (due to the close proximity of quencher and probe) effectively eliminates quencher-occupied sites as contributors to the intensity at long times. Only probes in sites vacant of quenchers are observed at long times and should thus have the same slope at long times in the semi-log plot as the decay in the absence of added quenchers,  $k_0$ . Curve fitting of the time-resolved fluorescence decays at the various quencher concentrations are also provided in Figure 7. The fits provide values for  $k_0$ ,  $k_q$ , and  $n$ . Plots of  $n$  vs [DBA] yield the linear plot of Figure 8, the slope of which is equal to  $1/[\text{site}]$ , thus providing another estimate of  $N$ . Small amounts of pyrene in a polar environment may be responsible for slight nonlinearity near the origin as discussed later; this contribution is neglected in the present analysis as the deviations from linearity are small. A summary of the Poisson kinetics results are provided in Table II. There is good agreement between transient and steady-state measurements. The results from the transient fits are slightly lower than those from steady-state measurements due to a nominal static component in the quenching kinetics. The static component is not included in the fitting

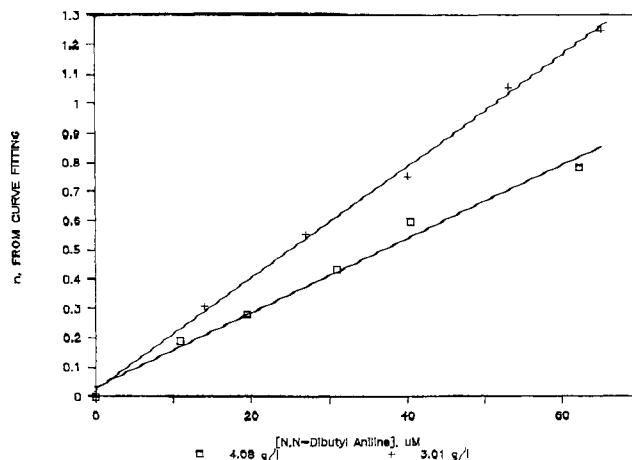


**Figure 8.** Time-resolved quenching of pyrene by  $N,N$ -dibutylaniline in P(AM/STY)-22 solutions. At both 4.08 and 3.01 g/L copolymer, pyrene concentrations are  $5 \times 10^{-6}$  M. At each quencher concentration the parameter,  $n$  ( $n = [Q]/[\text{sites}]$ ) permits calculation of site size; the least-squares slope of  $n$  vs  $[Q]$  yields an estimate of site size of  $N = 19$  sty/site for P(AM/STY)-22.

of the decays that could slightly lower the determined  $n$  values. However, the agreement between steady-state and transient values for  $N$  are evaluated to be within the limits of these photophysical methods. Also, the determined values of  $N$  are very close to calculated values for the  $[\text{sty}]/[\text{micelles}]$  ratios calculated in the reaction mixtures indicating that the micellar polymerization technique precisely controls the styrene block sizes.

With sites of average size as low as about 13 styrenes per site, it seems unreasonable to expect such small sites to protect solubilized pyrene from the polar quenchers, despite their apparent rigidity. However, it is unlikely that the sites are composed entirely of only styrene monomers. Again, in Figure 1, the presence of monomer polystyrene emission from the copolymers indicates at least some of the styrene has some acrylamide interspersed so that if almost all of the styrenes are involved in the formation of the sites, the sites could be substantially larger. One might therefore expect a change in penetrability of the sites with copolymer concentration, but no such effect is observed. An additional possibility involves the configuration of the polyacrylamide backbone in the vicinity of the styrene blocks. The acrylamide chains may coil about the styrene blocks, impeding interaction with the aqueous phase and facilitating solubilization of the copolymers in water. The results of Figure 5 support the postulated coiled configuration in that there is only a nominal dependence in the accessibility of pyrene by nitromethane on the size of the styrene blocks. With a coiled configuration, there should be little difference in the overall size of the effective hydrophobic sites in each of the different copolymers. Thus, part of the protective nature seemingly can be attributed to an outer core of polyacrylamide that is present for each block size measured. In addition, the curvature seen at low [NM] in Figure 5 is suggestive of dual environments for solubilized pyrene. A distribution of probes between two distinct environments of unequal accessibility can account for the noted curvature. The lifetime of pyrene emission in a polyacrylamide film (190 ns) is roughly half that in a polystyrene film ( $\sim 400$  ns) which provides a clue to the nature of the two environments: A coiled configuration with the polyacrylamide backbone surrounding the polystyrene blocks would be consistent with the noted anomalies in pyrene accessibility and environment.

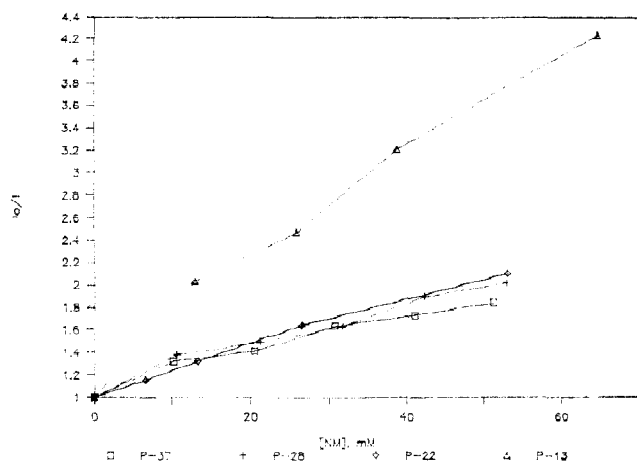


**Figure 9.** Quenching of pyrene by nitromethane in hydrolyzed block copolymers at pH = 3.0. Copolymer concentrations are 4 g/L with  $5 \times 10^{-6}$  M pyrene.

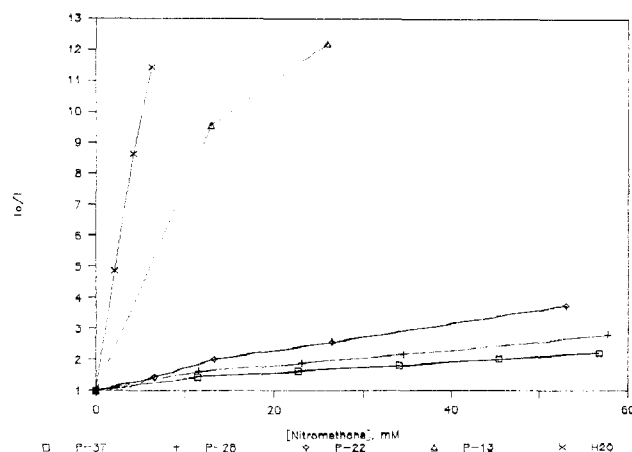


**Figure 10.** Quenching of pyrene by nitromethane in hydrolyzed block copolymers at pH = 7.5. Copolymer concentrations are 4 g/L with  $5 \times 10^{-6}$  M pyrene.

**Hydrolyzed Copolymers.** Confirmation that chain coiling is responsible for contributing to the hydrophobic host sites is evident in the changes in accessibility observed upon chemical alteration of the polymer. Hydrolysis of the polyacrylamide backbone to its poly(acrylic acid) (PAA) derivative does not significantly affect styrene block size as determined by the Poisson counting method but appreciably alters the accessibility of solubilized pyrene by nitromethane, as displayed in Figures 9 and 10. Two trends are worth noting: (1) the accessibility of pyrene at high pH (pH  $\sim 7.5$ ) becomes strongly dependent on the size of the styrene blocks, and (2) the quenching of pyrene by nitromethane develops a dependence upon pH for a given block size not evident in the precursor copolymers. This second trend is most pronounced for the smallest block sizes.

For several decades it has been known that PAA undergoes conformational changes as a function of pH.<sup>18</sup> An open structure exists at high pH due to the electrostatic repulsion of neighboring negative charges. A coiled, slightly hydrophobic structure exists at low pH as the acidic form predominates. In the P(AA/Sty)-hydrolyzed derivative block copolymers, the accessibility of pyrene is enhanced at high pH in comparison to that at low pH (pH  $\sim 3.0$ ) and the P(AM/Sty) precursor solutions for each copolymer. These differences are consistent with the known behavior of PAA with pH only if the polymer backbone contributes to the screening of the pyrene from the aqueous phase in the low pH and nonhydrolyzed precursor

copolymers; at low pH, coiling about hydrophobic centers can occur to contribute to the screening effect, whereas, at high pH, the screening is decreased by an opening of the chain. The large dependence of pyrene accessibility upon the styrene block size at high pH (Figure 10) underscores the important role the polymer backbone plays in the screening. In the nonhydrolyzed precursors and the low pH solutions of the hydrolyzed derivatives, block size is relatively unimportant in determining the degree of screening. However, at high pH the open structure renders the styrene block alone as the predominant protection for the probe from aqueous quenchers.

## Conclusions

Kinetics of fluorescence evaluated in terms of the Poisson distribution demonstrate that block copolymers of acrylamide and styrene may be prepared in a micellar medium for the control of styrene block sizes. Hydrophobic domains arise as a result of the styrene blocks and provide an environment for solubilized molecules that is largely protected from the aqueous phase. Chain configuration contributes to the host site, as the degree of isolation from the aqueous phase is virtually independent of the block size, prior to hydrolysis of the P(AM/Sty) copolymers. Consequently, the accessibility of pyrene in the host sites of the hydrolyzed derivatives show a large dependence on solution pH and on the styrene block sizes at high pH.

**Acknowledgment.** We wish to thank the National Science Foundation, via Grant CHE-89-11-906, for support of this work.

## References and Notes

- (1) Fendler, J. H. *Membrane Mimetic Chemistry*; Wiley-Interscience: New York, 1982.
- (2) Turro, N. J.; Gratzel, M.; Braun, A. M. *Angew. Chem., Int. Ed. Engl.* **1980**, *19*, 675.
- (3) Winnik, M. A. In *Polymer Surfaces and Interfaces*; Wiley: New York, 1987.
- (4) Thomas, J. K. *The Chemistry of Excitation at Interfaces*; American Chemical Society: Washington, DC, 1984.
- (5) Gros, L.; Ringsdorf, H.; Schupp, H. *Angew. Chem., Int. Ed. Engl.* **1981**, *20*, 305.
- (6) McCormick, C. L.; Nonaka, T.; Johnson, C. B. *Polymer* **1988**, *29*, 731.
- (7) Turro, N. J.; Kuo, P. J. *J. Phys. Chem.* **1986**, *90*, 4205.
- (8) Nagarajan, R.; Barry, M.; Ruckenstein, E. *Langmuir* **1986**, *2*, 210.
- (9) Ruckenstein, E.; Park, J. S. *J. Polym. Sci., Polym. Lett. Ed.* **1988**, *26*, 529.
- (10) Turro, N. J.; Kuo, P. L. *Macromolecules* **1987**, *20*, 1216.
- (11) Thomas, J. K.; Murtagh, J.; Ferrick, M. R. *Macromolecules* **1989**, *22*, 1515.
- (12) Thomas, J. K.; Hashimoto, S. *J. Am. Chem. Soc.* **1985**, *107*, 4655.
- (13) Collinson, E.; Dainton, F. S.; McNaughton, G. S. *Trans. Faraday Soc.* **1957**, *53*, 489.
- (14) Ananthapadmanabhan, K. P.; Goddard, E. D.; Turro, N. J.; Kuo, P. L. *Langmuir* **1985**, *1*, 352.
- (15) Kalyanasundaram, K.; Thomas, J. K. *J. Am. Chem. Soc.* **1977**, *99*, 2039 and references therein.
- (16) Azumi, T.; McGlynn, S. P. *J. Chem. Phys.* **1962**, *37*, 2413.
- (17) Kalyanasundaram, K. *Photochemistry in Microheterogeneous Systems*; Academic Press: Orlando, FL, 1987.
- (18) Katchalsky, A.; Eisenberg, H. *J. Polym. Sci.* **1951**, *6*, 145.
- (19) Mukerjee, P.; Mysels, K. J. *Critical Micelle Concentrations of Aqueous Surfactant Systems*; NSRDS-NBS: Washington, DC, 1970.